

**Original data for "Multiple co-existing structures of an RNA four-way junction resolved by FRET, SAXS, and integrative modeling " describing the major state**

Christian A. Hanke, Hayk Vardanyan, Simon Sindbert, Stanislav Kalinin, Anders Barth, Mykola Dimura, Tomasz Soltysinski, Grzegorz Lach, Danilo Springstube, Bettina Apel, Edward Snell, Thomas D. Grant, Jan Lipfert, Sabine Müller, Janusz M. Bujnicki, Holger Gohlke, Claus A. M. Seidel<sup>1</sup>

<sup>1</sup> Contact: Lehrstuhl für Molekulare Physikalische Chemie, Heinrich-Heine-Universität Düsseldorf, Universitätsstr. 1, 40225 Düsseldorf, Germany; e-mail: cseidel@hhu.de

The following files are available on Zenodo under DOI [10.5281/zenodo.6640962](https://doi.org/10.5281/zenodo.6640962)

- \* Starting structures for rigid body docking in the folder "Rigid\_Body\_Docking\_Starting\_structures"
- \* Intensity ratio histograms for measurements on the RNA four-way junction (RNA4WJ) in the folder "Intensity\_ratio\_histogram\_data"

The following intensity ratio histograms are uploaded:

Filename	Content
b5D_a12A_data.txt	Intensity ratio histogram for variant b5D_a12A
b5D_d10A_data.txt	Intensity ratio histogram for variant b5D_d10A
b5D_d23A_data.txt	Intensity ratio histogram for variant b5D_d23A
b5D_d26A_data.txt	Intensity ratio histogram for variant b5D_d26A
b5D_c8A_data.txt	Intensity ratio histogram for variant b5D_c8A
b5D_c24A_data.txt	Intensity ratio histogram for variant b5D_c24A
b8D_a12A_data.txt	Intensity ratio histogram for variant b8D_a12A
b8D_d10A_data.txt	Intensity ratio histogram for variant b8D_d10A
b8D_d23A_data.txt	Intensity ratio histogram for variant b8D_d23A
b8D_d26A_data.txt	Intensity ratio histogram for variant b8D_d26A
b8D_d28A_data.txt	Intensity ratio histogram for variant b8D_d28A
b8D_c8A_data.txt	Intensity ratio histogram for variant b8D_c8A
b8D_c24A_data.txt	Intensity ratio histogram for variant b8D_c24A
b11D_a12A_data.txt	Intensity ratio histogram for variant b11D_a12A
b11D_d10A_data.txt	Intensity ratio histogram for variant b11D_d10A
b11D_d23A_data.txt	Intensity ratio histogram for variant b11D_d23A
b11D_d26A_data.txt	Intensity ratio histogram for variant b11D_d26A
b11D_d28A_data.txt	Intensity ratio histogram for variant b11D_d28A
b11D_c8A_data.txt	Intensity ratio histogram for variant b11D_c8A
b11D_c24A_data.txt	Intensity ratio histogram for variant b11D_c24A
b14D_a12A_data.txt	Intensity ratio histogram for variant b14D_a12A
b14D_d10A_data.txt	Intensity ratio histogram for variant b14D_d10A
b14D_d23A_data.txt	Intensity ratio histogram for variant b14D_d23A
b14D_d26A_data.txt	Intensity ratio histogram for variant b14D_d26A
b14D_d28A_data.txt	Intensity ratio histogram for variant b14D_d28A
b14D_c8A_data.txt	Intensity ratio histogram for variant b14D_c8A
b14D_c24A_data.txt	Intensity ratio histogram for variant b14D_c24A
b27D_d10A_data.txt	Intensity ratio histogram for variant b27D_d10A
b27D_d23A_data.txt	Intensity ratio histogram for variant b27D_d23A
b27D_d26A_data.txt	Intensity ratio histogram for variant b27D_d26A
b27D_d28A_data.txt	Intensity ratio histogram for variant b27D_d28A
b27D_c24A_data.txt	Intensity ratio histogram for variant b27D_c24A
d7D_a12A_data.txt	Intensity ratio histogram for variant d7D_a12A
d7D_b14A_data.txt	Intensity ratio histogram for variant d7D_b14A
d7D_b27A_data.txt	Intensity ratio histogram for variant d7D_b27A

d7D_b33A_data.txt	Intensity ratio histogram for variant d7D_b33A
d7D_c8A_data.txt	Intensity ratio histogram for variant d7D_c8A
c8D_a12A_data.txt	Intensity ratio histogram for variant c8D_a12A
c8D_b14A_data.txt	Intensity ratio histogram for variant c8D_b14A
c8D_d10A_data.txt	Intensity ratio histogram for variant c8D_d10A
c8D_d23A_data.txt	Intensity ratio histogram for variant c8D_d23A
c8D_d26A_data.txt	Intensity ratio histogram for variant c8D_d26A
c8D_d28A_data.txt	Intensity ratio histogram for variant c8D_d28A
c29D_a12A_data.txt	Intensity ratio histogram for variant c29D_a12A
c29D_b14A_data.txt	Intensity ratio histogram for variant c29D_b14A
c29D_b27A_data.txt	Intensity ratio histogram for variant c29D_b27A
c29D_b33A_data.txt	Intensity ratio histogram for variant c29D_b33A
c29D_d23A_data.txt	Intensity ratio histogram for variant c29D_d23A
c29D_d26A_data.txt	Intensity ratio histogram for variant c29D_d26A
c29D_d28A_data.txt	Intensity ratio histogram for variant c29D_d28A

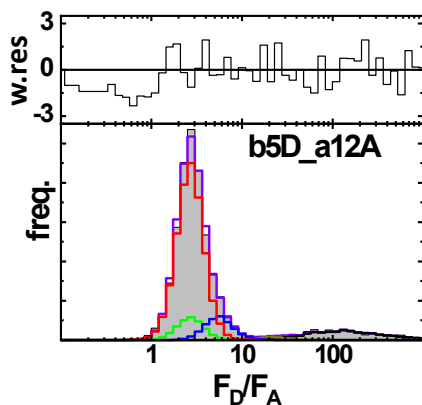
Note on naming of FRET pairs:

Example b5D\_a12A: The donor fluorophore (D) is attached at position 5 on strand b, and the acceptor fluorophore (A) is attached to position 12 on strand a.

### Explanation of Intensity ratio histogram data

The experimental FRET data was processed using photon distribution analysis (PDA) [1,2].

The experimental  $F_D/F_A$  histograms (gray areas in the picture) is fitted (purple solid line) with three FRET populations.  $\langle R_{DA} \rangle_{E(1)}$  in red for the major state  $(ad)_a$ ,  $\langle R_{DA} \rangle_{E(2)}$  in green for the second FRET population, and  $\langle R_{DA} \rangle_{E(3)}$  in blue for the third FRET population), one donor-only (D-only in black) and one impurity state (dark yellow). Weighted residuals (w.res) for the fit are show in the upper panel.



The format of the Data files is as follows:

Column number	1	2	3	4	5	6	7	8	9
	Experimental data		Model						Experiment - model
Axes	X	Y	Y	Y	Y	Y	Y	Y	Y
Content	$F_D/F_A$ (corrected)	Experiment_Histogram	Fit	D-only	Impurity_state	Major_state(ad)_a	FRET_population_2	FRET_population_3	w.res
Units	N/A	Counts	Counts	Counts	Counts	Counts	Counts	Counts	Counts

Fractions for the Intensity ratio histogram fit with three FRET populations and the corrections parameters used [3] for the fits<sup>a</sup>.

DA-pair	$x_1$ [%]	$x_2$ [%]	$x_3$ [%]	$x_{D-only}$ [%]	$x_{impurities}$ [%]	$\langle B_G \rangle$ [kHz]	$\langle B_R \rangle$ [kHz]	$\alpha$ [%]	$g_G/g_R$	$\chi_r^2$
b5D_a12A	62.1	8.0	8.6	20.0	1.3	1.19	0.79	2.40	0.40	1.48
b5D_c8A	39.6	6.6	7.7	44.0	2.1	1.13	0.75	2.20	0.40	0.78
b5D_c24A	51.4	8.4	8.4	28.7	2.9	1.54	0.59	1.30	0.73	1.48
b5D_d10A	43.3	14.5	11.4	28.0	2.8	1.95	0.64	1.20	0.71	2.32
b5D_d23A	32.7	5.2	10.6	51.5	0.0	1.19	0.79	2.40	0.40	1.36
b5D_d26A	56.7	7.5	8.3	26.3	1.3	0.99	0.67	3.00	0.32	1.17
b8D_a12A	59.0	9.4	11.6	18.9	1.1	1.13	0.75	2.50	0.40	1.14
b8D_c8A	47.1	8.2	9.3	32.8	2.6	1.29	0.55	1.30	0.70	1.99
b8D_c24A	42.5	7.6	14.0	35.8	0.0	1.81	0.75	1.40	0.74	2.4
b8D_d10A	24.2	9.8	5.8	57.6	1.7	1.81	0.75	1.30	0.74	0.78
b8D_d23A	38.5	12.3	5.4	42.0	1.8	1.3	0.54	1.40	0.85	0.84
b8D_d26A	46.1	15.4	15.4	21.0	2.2	0.99	0.67	2.60	0.32	0.98
b8D_d28A	58.2	8.8	8.8	23.0	1.2	1.3	0.54	1.40	0.85	0.67
b11D_a12A	67.1	7.6	3.7	20.8	0.8	1.13	0.75	2.30	0.40	0.97
b11D_c8A	46.9	6.2	6.7	38.6	1.6	1.57	0.69	1.30	0.80	1.38
b11D_c24A	59.4	4.9	7.9	26.4	1.3	1.74	0.64	1.40	0.71	1.73
b11D_d10A	64.8	6.7	7.9	19.7	0.9	1.74	0.64	1.50	0.71	1.32
b11D_d23A	45.1	4.9	11.9	36.2	1.9	1.66	0.65	1.30	0.67	1.88
b11D_d26A	64.7	8.4	8.4	18.5	0.0	0.99	0.67	2.60	0.32	1.05
b11D_d28A	62.5	6.0	6.0	22.6	3.0	1.29	0.55	1.20	0.70	0.78
b14D_a12A	62.1	8.6	8.6	19.0	1.8	1.13	0.75	2.90	0.40	3.05
b14D_c8A	47.0	3.8	6.2	41.5	1.5	1.57	0.69	1.30	0.80	1.42
b14D_c24A	32.5	12.6	11.9	41.7	1.3	1.73	0.72	1.40	0.74	1.22
b14D_d10A	35.5	12.7	13.0	37.7	1.0	1.73	0.72	1.90	0.74	1.69
b14D_d23A	31.7	9.5	9.5	45.9	3.5	1.29	0.54	1.50	0.85	1.5
b14D_d26A	39.1	5.5	5.5	47.2	2.8	1.19	0.79	2.70	0.40	0.78
b14D_d28A	49.8	12.4	9.6	27.0	1.3	1.3	0.54	1.30	0.85	0.9
b27D_c24A	40.5	15.3	18.1	26.5	1.0	1.54	0.59	1.30	0.73	1.71
b27D_d10A	31.2	8.7	13.9	43.1	3.1	1.73	0.72	1.50	0.74	1.74
b27D_d23A	50.9	4.6	6.5	36.4	1.5	1.27	0.53	1.20	0.85	1.17
b27D_d26A	53.6	10.0	8.4	28.0	0.0	2.19	1.15	0.70	0.75	0.99
b27D_d28A	46.3	16.5	8.6	28.6	0.0	1.29	0.67	1.20	0.75	2.06
c8D_a12A	56.2	6.1	6.1	30.6	1.1	0.99	0.67	2.80	0.32	2.11
c8D_b14A	60.0	5.6	8.7	24.9	0.7	1.13	0.75	2.70	0.40	1.06
c8D_d10A	56.6	11.5	5.4	24.0	2.5	1.73	0.72	1.50	0.73	0.83
c8D_d23A	31.0	3.5	4.6	60.1	0.9	0.99	0.67	2.60	0.32	0.68
c8D_d26A	51.9	2.7	8.4	33.6	3.4	1.44	0.99	2.20	0.40	1.29
c8D_d28A	54.0	4.2	8.0	32.1	1.6	1.83	0.79	1.40	0.67	1.51
c29D_a12A	66.5	8.0	3.1	20.0	2.5	1.44	0.99	2.30	0.40	1.89
c29D_b14A	59.5	2.2	9.3	25.9	3.1	1.27	0.53	1.50	0.85	1.2
c29D_b27A	44.6	4.9	14.7	33.3	2.5	1.43	0.62	2.00	0.80	1.03
c29D_b33A	55.5	5.6	7.7	28.4	2.8	1.43	0.62	1.90	0.80	1.42
c29D_d23A	65.7	7.9	3.8	22.6	0.0	1.57	0.69	1.30	0.80	1.25
c29D_d26A	51.4	20.4	2.7	25.6	0.0	1.44	0.99	2.30	0.40	0.7
c29D_d28A	58.1	8.9	8.9	24.2	0.0	1.57	0.69	1.30	0.80	1.75
d7D_a12A	51.1	10.7	10.7	26.7	8.0	1.12	0.73	3.20	0.35	1.78
d7D_b14A	57.9	4.1	3.8	33.1	1.0	1.42	0.61	1.60	0.80	1.02
d7D_b27A	38.4	7.8	11.6	38.7	3.5	1.43	0.62	1.90	0.80	1.21
d7D_b33A	57.0	10.6	16.3	13.7	2.3	1.5	0.56	1.50	0.69	2.11
d7D_c8A	41.4	10.2	10.2	37.1	1.0	1.29	0.67	1.30	0.75	2.74

<sup>a</sup> With  $x_1$ ,  $x_2$ ,  $x_3$  the fractions of the three FRET populations,  $x_{D-only}$  the fraction of the donor-only population,  $x_{impurities}$  the fraction of the impurities,  $\langle B_G \rangle$  and  $\langle B_R \rangle$  the background counts in the green and red channel,  $\alpha$  the correction factor,  $g_G/g_R$  the detection efficiency ratio, and  $\chi_r^2$  the quality parameter for the fit.

Quantum yields  $\Phi_{FD}$  and  $\Phi_{FA}$  for the labeling positions

Labeling position	$\Phi_{FD}$
b5D	0.76
b8D	0.68
b11D	0.71
b14D	0.75
b27D	0.61
c8D	0.66
c29D	0.52
d7D	0.65

Labeling position	$\Phi_{FA}$
a12A	0.33
b14A	0.33
b27A	0.32
b33A	0.46
c8A	0.34
c24A	0.32
d10A	0.35
d23A	0.31
d26A	0.41
d28A	0.47

#### References:

- [1] Antonik, M., Felekyan, S., Gaiduk, A. & Seidel, C. A. M. Separating structural heterogeneities from stochastic variations in fluorescence resonance energy transfer distributions via photon distribution analysis. J. Phys. Chem. B 110, 6970-6978 (2006).
- [2] Kalinin, S., Felekyan, S., Valeri, A. & Seidel, C. A. M. Characterizing multiple molecular states in single-molecule multiparameter fluorescence detection by probability distribution analysis. J. Phys. Chem. B 112, 8361-8374 (2008).
- [3] Sisamak, E., Valeri, A., Kalinin, S., Rothwell, P. J., Seidel, C. A. M. Accurate single-molecule FRET studies using multiparameter fluorescence detection. Methods in Enzymology 475, Chapter 18, 455-514 (2010).